Journal of Geochemical Exploration xxx (2015) xxx–xxx

Contents lists available at ScienceDirect

Journal of Geochemical Exploration

journal homepage: www.elsevier.com/locate/jgeoexp

Spatial distribution of arsenic, uranium and vanadium in the volcanic-sedimentary aquifers of the Vicano–Cimino Volcanic District (Central Italy)

D. Cinti[a,*], P.P. Poncia[b], L. Brusca[c], F. Tassi[d,e], F. Quattrocchi[a], O. Vaselli[d,e]

[a] Istituto Nazionale di Geofisica e Vulcanologia (INGV), Via di Vigna Murata, 605-00143 Roma, Italy
[b] Po Valley Operations PTY Ltd, via Ludovisi 16, 00187 Roma, Italy
[c] Istituto Nazionale di Geofisica e Vulcanologia (INGV), Via U. La Malfa, 153-90146 Palermo, Italy
[d] Dipartimento di Scienze della Terra, Università di Firenze, via G. La Pira 4, 50121 Firenze, Italy
[e] CNR - Istituto di Geoscienze e Scienze della Terra, via G. La Pira 4, 50121 Firenze, Italy

ARTICLE INFO

Article history:
Received 23 September 2014
Accepted 16 February 2015
Available online xxxx

Keywords:
Arsenic
Uranium
Vanadium
Central Italy
Volcanic–sedimentary aquifers
Geostatistical techniques

ABSTRACT

Arsenic concentrations were analysed for 328 water samples collected in the Vicano–Cimino Volcanic District (VCVD), an area where severe contamination of groundwater has become a serious problem following the recent application of the EU Directive on the maximum allowable concentration level for As in drinking waters. In addition, uranium and vanadium concentrations were also analysed in light of the enhanced interest on their environmental toxicity. Waters were collected from springs and wells fed by cold and shallow volcanic–sedimentary aquifers, which locally represent the main drinking water source. Thermal springs (≤63 °C) related to an active hydrothermal reservoir and waters associated with a CO_2-rich gas phase of deep provenance were also analysed. The collected data showed that the As concentrations in the shallow aquifers varied in a wide range (0.05–300 μg/L) and were primarily controlled by water–rock interaction processes. High As concentrations (up to 300 μg/L) were measured in springs and wells discharging from the volcanic products, and about 66% exceeded the limit of 10 μg/L for drinking waters, whereas waters circulating within the sedimentary formations displayed much lower values (0.05–13 μg/L; ~4% exceeding the threshold limit). Thermal waters showed the highest As concentrations (up to 610 μg/L) as the result of the enhanced solubility of As-rich volcanic rocks during water–rock interaction processes at high temperatures. Where the local structural setting favoured the rise of fluids from the deep hydrothermal reservoir and their interaction with the shallow volcanic aquifer, relatively higher concentrations were found. Moreover, well overexploitation likely caused the lateral inflow of As-rich waters towards not contaminated areas.

Uranium and vanadium concentrations of waters circulating in the volcanic rocks ranged from 0.01 to 85 μg/L and 0.05 to 62 μg/L, respectively. Less than 2% of analysed samples exceeded the World Health Organization's provisional guidelines for U (30 μg/L), while none of them was above the Italian limit value of V in drinking water (120 μg/L). Lower U (0.07–22 μg/L and 0.02–13 μg/L, respectively) and V concentrations (0.05–24 μg/L and 0.18–17 μg/L, respectively) were measured in the water samples from the sedimentary aquifer and thermal waters. Local lithology appeared as the main factor affecting the U and V contents in the shallow aquifers, due to the high concentrations of these two elements in the volcanic formations when compared to the sedimentary units. In addition, high U concentrations were found in correspondence with U mineralization occurring within the VCVD, from which U is released in solution mainly through supergene oxidative alteration. Redox conditions seem to play a major role in controlling the concentrations of U and V in waters. Oxidizing conditions characterizing the cold waters favour the formation of soluble U- and V-species, whereas thermal waters under anoxic conditions are dominated by relatively insoluble species. Geostatistical techniques were used to draw contour maps by using variogram models and kriging estimation aimed to define the areas of potential health risk characterized by As, U and V-rich waters, thus providing a useful tool for water management in a naturally contaminated area to local Authorities.

1. Introduction

The peri-Tyrrhenian sector of central and southern Italy is a region of preferential release of naturally occurring toxic trace elements from Plio-Quaternary volcanic rocks into groundwater (Aiuppa et al., 2006;

* Corresponding author. Fax: +39 06 51860507.
E-mail address: daniele.cinti@ingv.it (D. Cinti).

http://dx.doi.org/10.1016/j.gexplo.2015.02.008
0375-6742/

Dall'Aglio et al., 2001; Dinelli et al., 2010; Giammanco et al., 1996; Tamasi and Cini, 2004; Vivona et al., 2007), a process enhanced by extensive thermalism (Cataldi et al., 1995) and the presence of reactive gas species (e.g. CO_2, H_2S) (Chiodini et al., 1999; Minissale, 2004). Since the last decade, understanding the geochemical processes that favour the occurrence of high As contents in large groundwater reservoir of central-Italy used for drinkable waters represents one of the main targets for the Italian scientific community (e.g. Angelone et al., 2009; Baiocchi et al., 2013) and policy-makers, as the maximum allowable concentration in water intended for human consumption was lowered from 50 to 10 μg/L (EC Directive, 1998). Episodes of severe As contamination of drinking waters were reported in several countries (e.g. India, Argentina, Chile, Mexico, etc.) from naturally affected areas (e.g. Katsoyiannis et al., 2007; Rahman et al., 2005; Romero et al., 2003; Smedley and Kinniburgh, 2002; Smedley et al., 2005) together with its effects on human health, which include cardiovascular, renal, haematological and respiratory disorders and also skin and internal (bladder, lung, prostate) cancers (IARC, 2004). Arsenic is sensitive to mobilization at the pH values typically found in ground waters (6.5–8.5) and under both oxidizing and reducing conditions (Smedley and Kinniburgh, 2002). Arsenic is mostly occurring in solution in inorganic form as oxyanions of trivalent arsenite As(III) or pentavalent arsenate As(V) (e.g. Smedley and Kinniburgh, 2002). As-rich waters are commonly associated with 1) the presence of active geothermal systems (e.g. Aiuppa et al., 2006; Ballantyne and Moore, 1988; Webster and Nordstrom, 2003) and 2) enhanced water–rock interaction processes in different stratigraphic and hydrogeochemical settings (e.g. Smedley and Kinniburgh, 2002, and references therein). Anthropogenic processes responsible for As contamination of water are mainly related to mining activities, combustion of fossil fuels and use of arsenical pesticides and herbicides (Smedley and Kinniburgh, 2002).

Uranium was recognized as a toxic contaminant of groundwater since 1998. In 2011, a provisional health-based U guideline concentration of 30 μg/L was promulgated by the World Health Organization (WHO, 2011) for drinking waters, since they represent the primary source of U intake for humans. Although the naturally occurring U is radioactive, the overall risks arising from the biochemical toxicity of U as a heavy metal are considered to be about six orders of magnitude higher than those derived from its radioactivity (Milvy and Cothern, 1990). Effects of U intake in humans include kidneys disease (nephritis), increased risk related to fertility problems and reproductive cancers (EFSA, 2009). High U concentrations in groundwater were reported in many areas worldwide (e.g. Cicchella et al., 2010; Frengstad et al., 2000; Nriagu et al., 2012; Smedley et al., 2006; Wu et al., 2014), especially in the presence of U-rich granitic terrains and U-mineralized areas. Nevertheless, significant enrichments were also recorded in waters interacting with iron oxides, phosphates, clays and organic matter (Smedley et al., 2006 and references therein). Uranium is a redox-sensitive heavy metal that occurs in oxic waters, mostly as hexavalent U(VI), where uranyl ion (UO_2^{2+}) is the dominant form at low pH (<5), whereas at higher pHs carbonate complexes predominate (Smedley et al., 2006; Wu et al., 2014). Under anoxic conditions, U is reduced to its tetravalent form U(IV) and its concentration in water is relatively low as a result of stabilization of the sparingly soluble mineral uraninite (UO_2). Anthropogenic sources include mining activities, nuclear industry and fertilizer manufacture (Smedley et al., 2006).

Increasing interest on the toxicological effects of the ingestion of V from drinking water has grown in the last years. A number of studies have warned on the possible harmful effects of V when present at high concentrations (e.g. Gerke et al., 2010; Wright et al., 2014), leading the U.S. Environmental Protection Agency to list V in the Contaminant Candidate List 3 (USEPA, 2009). However, the toxicological studies are not fully exhaustive and the daily intake of V via drinking water is generally low. Consequently, V has not been yet considered by WHO as a contaminant. As far as contaminant regulation in Italy is concerned, the limit value of V in drinking water was increased from 50 to 120 μg/L, and a new parametric value of 140 μg/L was recently proposed (Crebelli and Leopardi, 2012). Potential natural sources of V in groundwater are related to rock weathering and sediment leaching, while anthropogenic sources include waste streams from industrial processes and iron pipe corrosion by-products (Dinelli et al., 2012; Gerke et al., 2010; Giammanco et al., 1996; Pourret et al., 2012). The behaviour of V in the aquatic environment is mainly regulated by redox and pH of the aqueous system (Wright et al., 2014). Under oxic conditions V is present as pentavalent V(V) and occurs in the oxyanionic form at pH values typically found in ground waters, whereas under reducing conditions the less soluble trivalent V(III) and tetravalent V(IV) species dominate.

In this study, 328 water samples from springs, private domestic and municipal wells, mostly used for human consumption, were collected from the Vicano–Cimino Volcanic District (VCVD) and analysed for As, U and V concentrations. Thermal and cold waters associated with a CO_2-rich bubbling gas phase, which are relatively common in the peri-Tyrrhenian sector of central Italy (Chiodini et al., 1999; Minissale, 2004), were also analysed. The main aims were to i) investigate the source of As, U and V and the main factors controlling their chemical behaviour in this natural environment and ii) reconstruct the spatial distribution of their concentrations and evaluate the potential health risk for areas affected by anomalous contamination.

2. Geodynamic, hydrogeological and petrological settings

VCVD is located along the peri-Tyrrhenian sector of central Italy, between the Tyrrhenian coast and the Apennine chain (Fig. 1). This sector has undergone a post-collisional Plio-Quaternary extensional phase, that led to a strong crustal thinning (<25 km; Scrocca et al., 2003) and generated heat flow anomalies (locally higher than 200 mW/m^2; Barberi et al., 1994; Cataldi et al., 1995) and subduction-related magmatism (Barberi et al., 1994; Peccerillo, 1985). Extensional tectonics formed preferentially NW–SE oriented horst and graben structures with clastic marine sediments filling the structural lows (Barberi et al., 1994).

The Cimino and Vicano volcanic complexes belong to two different magmatic cycles, respectively: 1) the acid cycle, represented by SiO_2-rich magma of the Tuscan Magmatic Province and 2) the undersaturated K-alkaline cycle of the Roman Magmatic Province (Aulinas et al., 2011; Barberi et al., 1994; Perini et al., 2004; Sollevanti, 1983), respectively. The Cimino complex was active from 1.35 to 0.94 Ma (Nicoletti, 1969). It consists of a series of rhyodacitic domes and ignimbrites emplaced along a NW–SE trending fracture zone. At the end of the eruptive activity a central volcano, emitting latitic and olivine-latitic lavas, developed (Cimarelli and De Rita, 2006). The Vicano complex (0.42–0.09 Ma; Laurenzi and Villa, 1987) consists of a strato-volcano developed on a NW–SE elongated graben at the intersection with a NE–SW fracture, with a central caldera depression hosting Lake Vico. Alternating explosive and effusive phases, producing fall deposits, lava and pyroclastic flows, were followed by circum-caldera hydromagmatic and strombolian eruptions. The products of the Vicano complex are mainly leucitites, phono-tephrites and leucite-phonolites (Perini et al., 2004). The volcanic products overlie a sedimentary sequence that made up of, from top to bottom (Fig. 1): 1) a Plio-Pleistocene complex that includes conglomerates, sandstones and mudstones, 2) a Cretaceous–Oligocene(?) Ligurian and Sub-Ligurian units, referred hereinafter to as Ligurian s.l. and 3) Mesozoic carbonates overlying Triassic evaporites (Burano Fm.).

The Vicano–Cimino volcanites constitute a water reservoir limited by the low-permeability Plio-Pleistocene sedimentary complex and the Ligurian s.l., which act as aquicludes (Baiocchi et al., 2006; Capelli et al., 2005). A continuous basal unconfined aquifer and several perched aquifers of limited and discontinuous extent were identified in relation to the complex hydrostratigraphy that includes relatively high-permeability formations (i.e. ignimbrites and lava flows) alternated to

Please cite this article as: Cinti, D., et al., Spatial distribution of arsenic, uranium and vanadium in the volcanic-sedimentary aquifers of the Vicano–Cimino Volcanic Distric..., J. Geochem. Explor. (2015), http://dx.doi.org/10.1016/j.gexplo.2015.02.008

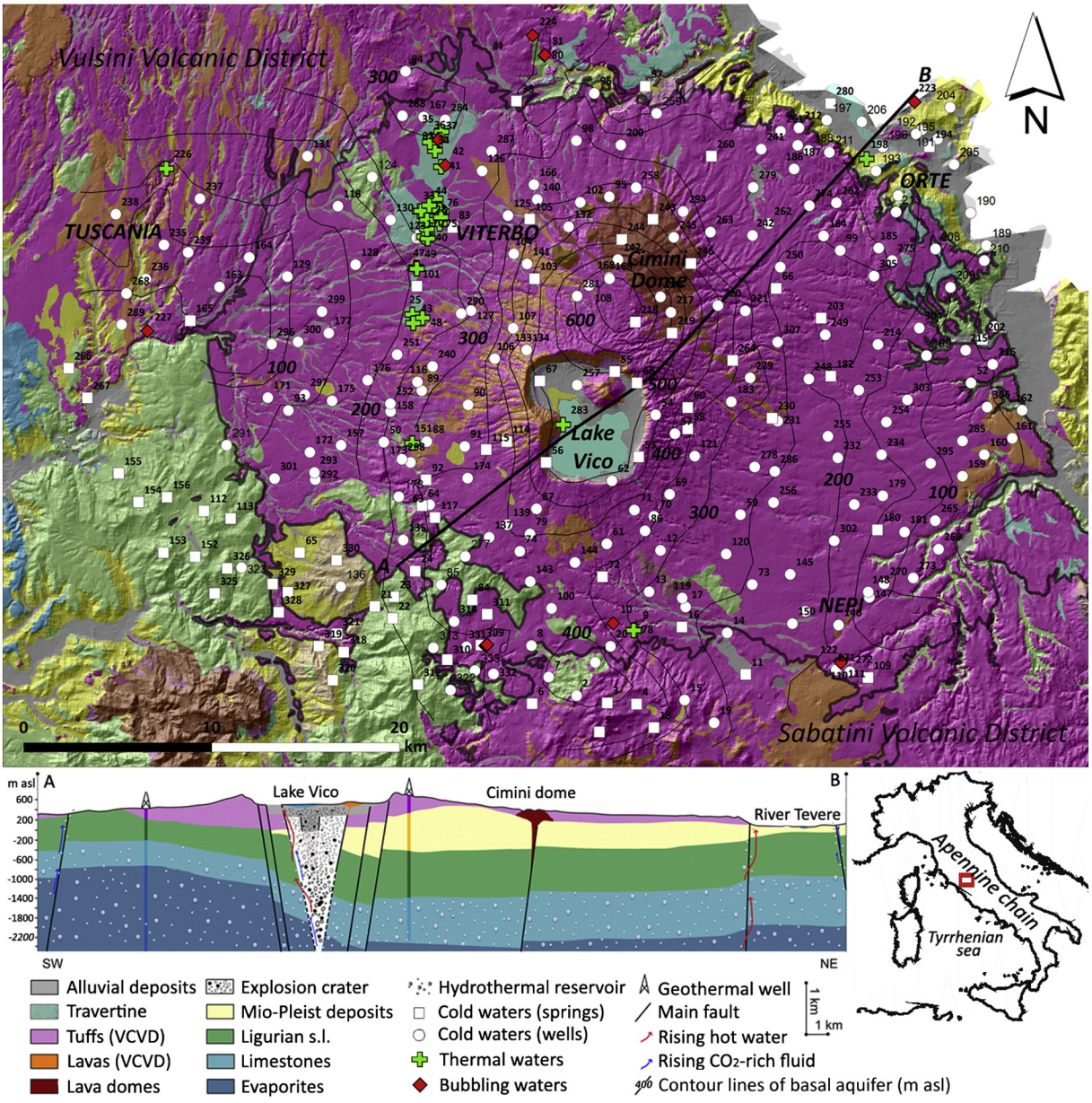

Fig. 1. Geological sketch map of the VCVD with the location of the sampled waters and interpretative cross-section indicating the groundwater circulation (modified after Cinti et al., 2014). The potentiometric surface of the basal aquifer is taken from Capelli et al. (2005) and Baiocchi et al. (2006).

low-permeability deposits (i.e. tuffs and fine-grained pyroclastic layers) (Baiocchi et al., 2006). Perched aquifers were also found in the permeable strata of the sedimentary deposits. The basal aquifer is characterized by radially divergent flow (Fig. 1). The potentiometric surface follows the topography, with the piezometric high in the central sector, the latter consisting of the Cimini Dome and the Lake Vico caldera (Fig. 1). Here, the surface of the lake corresponds to that of the basal unconfined aquifer (Baiocchi et al., 2006). The basal aquifer mainly discharges from springs with output flow <0.02 m^3/s. The perched aquifers both from volcanic and sedimentary deposits discharged from several springs, which are generally characterized by flow <0.005 m^3/s (Baiocchi et al., 2006). A regional hydrothermal aquifer hosted in the Mesozoic units was recognized at depth (Cinti et al., 2014). It is separated from the shallow continuous volcanic aquifer by low-permeability Plio-Pleistocene sedimentary complex and the Ligurian s.l. Fractures and faults affecting the sedimentary basement allow the uprising of thermal waters and CO_2-rich gases.

In such natural environment, the occurrence of potentially toxic elements in groundwater was mainly related to the weathering and dissolution of the volcanic rocks, whose composition is characterized by high contents of trace elements both in mineral structures and groundmass. Arsenic contents in the groundmass of lavas and pyroclastic deposits ranged from 34 to 180 ppm (parts per million) (Vivona et al., 2007). Very high U contents (up to 70 ppm) were measured in the volcanic products of the VCVD (Locardi and Mittempergher, 1971; Locardi and Sircana, 1967; Villemant and Fléoch, 1989). In addition, U-rich deposits were mainly found at the borders of the volcanic system, in correspondence with kaolinite alteration areas and in association with polymetallic sulphides and oxides. They were likely generated from secondary precipitation of U mobilized from the groundmass of the volcanic rocks (Capannesi et al., 2012; Locardi and Battistella, 1987; Locardi and Mittempergher, 1971; Rossi et al., 1995). Vanadium contents in the groundmass of lavas and pyroclastic layers ranged from 38 to 255 ppm (Aulinas et al., 2011; Perini et al., 2004). Stream sediments,

Please cite this article as: Cinti, D., et al., Spatial distribution of arsenic, uranium and vanadium in the volcanic-sedimentary aquifers of the Vicano–Cimino Volcanic Distric..., J. Geochem. Explor. (2015), http://dx.doi.org/10.1016/j.gexplo.2015.02.008

mostly originated from the outcropping volcanic rocks, and associated local mineralized areas also showed significant concentrations of As, U and V (mean values were 45, 3 and 76 ppm, respectively; Spadoni et al., 2005). In this respect, the sedimentary formations were poorly studied and chemical data are only available for U (Trevisi et al., 2005). The radiometric characterization of the different rock types showed significantly lower U concentrations for the sedimentary units (from 31 to 49 Bq/kg) relative to the volcanic rocks (from 134 to 160 Bq/kg).

3. Methods

Up to 328 water samples were collected over an area of approximately 1400 km^2 from cold and shallow springs and wells fed by 1) the aquifers hosted in the volcanic and sedimentary rocks and 2) the deep hydrothermal aquifer. Cold waters associated with a CO_2-rich bubbling gas phase released from the hydrothermal reservoir were also collected. The sampling sites were homogeneously distributed all over the investigated area (Fig. 1). Many springs and wells sampled from the shallow aquifers supply the local drinking water. The physical–chemical features of the studied waters and the composition of the main solutes were reported by Cinti et al. (2014). Samples for trace elements (As, U and V) analysis were collected in polyethylene bottles, which were pre-cleaned in the laboratory with diluted (1:3) Suprapur HNO_3 and then thoroughly rinsed with ultra-pure deionized water. Each sample was filtered with a 0.45 μm filter and then acidified to pH < 2 with ultra-pure HNO_3 to avoid metal precipitation and/or metal adsorption on the bottle surface. Elemental analyses were performed at Trace Elements Laboratory of INGV in Palermo (Italy) by inductively coupled plasma mass spectrometer (ICP-MS Agilent 7500ce) equipped with a Micromist nebulizer, a Scott double pass spray chamber, a three-channel peristaltic pump and an Octolpole Reaction System for removing interferences of polyatomic masses in Helium mode for Vanadium and Arsenic analyses. Before each measurement sequence, an auto-tune procedure was performed using a tuning solution for mass calibration, resolution, torch-position and electron multiplier calibration. This was followed by instrument optimization, nebulizer gas (argon) flow optimization, lens optimization, and an instrument performance check. The mass spectrometer was calibrated using external standards. Calibration solutions for all of the investigated elements were prepared daily using an appropriate dilution of 100 mg/L and 1000 mg/L of stock standard solutions (Merck) with 2% high-purity HNO_3 (Baker). The external standards concentrations for each element were chosen to encompass the anticipated elemental concentrations of samples in the ICP-MS analysis solution: 0.1–100 μg/L for V and As, and 0.01–10 μg/L for U. All standards and samples were replicated 5 times for precision evaluation. The accuracy of the method was checked analysing certified reference materials of natural waters (NIST 1643e, Environment Canada TM-24.3 and TM-61.2, Spectrapure Standards SW1 and SW2) at regular intervals during sample analysis. The experimental concentrations determined in this study were in accordance with these certified values (within 10%). Matrix induced signal suppressions and instrumental drift were corrected by internal standardization: we used indium for V and As correction and rhenium for U.

Descriptive statistics and graphical representations were carried out to characterize the population of water samples and all subsets with respect to As, U and V concentrations. Two different statistical tests were applied for data analysis: *i*) the Levene's test (Brown and Forsythe, 1974) to compare the variances of the distributions, and *ii*) the Kruskal–Wallis test to execute multiple comparison among subsets once the homogeneity of variances was verified and the assumption of normality was not acceptable (Kruskal and Wallis, 1952). After statistical analysis, the chemical data were processed to produce contour maps using a geostatistical approach (i.e. variogram analysis and kriging; Goovaerts, 1997). Kriging was applied to provide the best local estimate of the mean value of a regionalized variable (i.e. a certain property that varies in the geographic space) by using the measured values and a semi-variogram to determine the scale of variance and estimate unknown values. The geostatistical approach was used to: *i*) construct the experimental directional variograms for investigating the spatial dependence of the As, U and V concentrations (i.e. calculation of the main variogram parameters: nugget, range and sill), *ii*) determine the directional differences (anisotropy) for the kriging estimation (i.e. directions and ratio between the major and minor anisotropy ellipse axes), *iii*) model the experimental variograms using the geological information, *iv*) validate the selected model (i.e. cross-validation) for computing errors, thereby defining how well the model fits and *v*) estimate the spatial distribution of the studied variables using variogram model parameters in the kriging algorithm to construct contour maps.

4. Results

4.1. Basic statistics

Arsenic, U and V concentrations in the water samples (in μg/L) along with geographical coordinates, type of emergence and aquifer were provided as electronic Supplementary material (SM 1). Basic statistics (Table 1) show that samples are positively skewed (i.e. the average is higher than median value) for the three elements and, therefore, characterized by non-normal distribution. Arsenic concentrations ranged from 0.05 to 610 μg/L with a median value, which represents a more robust statistic parameter for non-normal distributions, of 13 μg/L and an inter-quartile range (IQR), representative of the distribution dispersion, of 24 μg/L (4.6–29 μg/L). Uranium concentrations varied from 0.01 to 280 μg/L, with a median value of 2.0 μg/L and IQR of 3.7 μg/L (0.66–4.4 μg/L). Vanadium concentrations were varying from 0.05 to 350 μg/L, with a median value of 8.9 μg/L and IQR of 12 μg/L (2.8–15 μg/L). The Pearson correlation matrix calculated on the entire dataset (see as electronic Supplementary material SM 2) shows no significant correlations among elements.

Four subsets of the whole population were defined on the basis of the water type (Table 1), as previously proposed by Cinti et al. (2014): 1) cold waters from the aquifer hosted in the volcanic rocks, 2) cold waters from the aquifer in the sedimentary deposits, 3) thermal waters and 4) bubbling pools (i.e. cold waters associated with a CO_2-rich bubbling gas phase). The main criterion for distinguishing between cold waters circulating within the volcanic and sedimentary formations was the outcropping unit at the sampling site (Fig. 1). Where such a condition demonstrated to be somewhat ambiguous (i.e. in the neighborhood of the contact of volcanic–sedimentary units) the chemical composition of waters (Cinti et al., 2014) was taken to distinguish samples belonging to one of the two groups. Frequency distributions are positively skewed for the selected subsets (Table 1), except for that of As concentrations in thermal waters, which is slightly negative. The Pearson correlation matrix calculated on the four subsets (see as electronic Supplementary material SM 3) shows a strong positive correlation between U and V in cold-sedimentary waters and bubbling pools and a minor correlation in cold-volcanic waters and thermal waters. As for arsenic, a slight correlation exists with U and V except for thermal waters where no correlation occurs. Box-plots (Fig. 2) graphically show, for each element analysed, the differences among the defined subsets. Up to 66% of waters from the volcanic aquifer showed As concentrations exceeding the value of 10 μg/L, and are characterized by higher concentrations and larger dispersions (median: 15 μg/L and IQR: 15 μg/L; Table 1) than those of the waters from the sedimentary aquifer (median: 0.42 μg/L and IQR: 2.6 μg/L), but lower than those of the thermal waters (median: 300 μg/L and IQR: 280 μg/L). Uranium concentrations were significantly higher in the waters from the volcanic aquifer (median: 2.8 μg/L and IQR: 4.2 μg/L) with respect to the other subsets, although less of 2% of samples exceeded the limit recommended by WHO (30 μg/L). The highest V concentrations were measured for those waters hosted in the volcanic aquifer (median: 12 μg/L and IQR:

Please cite this article as: Cinti, D., et al., Spatial distribution of arsenic, uranium and vanadium in the volcanic-sedimentary aquifers of the Vicano–Cimino Volcanic Distric..., J. Geochem. Explor. (2015), http://dx.doi.org/10.1016/j.gexplo.2015.02.008

Table 1
Basic statistics relative to 1) the whole population of samples, 2) subsets of the whole population were defined on the basis of the water type, 3) subsets of the volcanic and sedimentary water types defined on the basis the differences between wells and springs.

Arsenic	No. of observations	Min.	Max.	Q1	Median	Q3	Inter-quartile range	Average	Std-dev.	Skewness	Kurtosis
Whole population	328	0.05	610	4.6	13	29	24	44	95	3.2	10
Cold-volcanic	223	0.17	300	7.5	15	22	15	24	36	5.4	36
Cold-sedimentary	57	0.05	13	0.15	0.42	2.8	2.6	2.0	3.0	2.1	3.9
Thermal waters	33	0.08	610	77	300	360	280	250	160	−0.19	−0.74
Bubbling pools	15	0.05	390	0.58	2.6	14	14	38	98	3.1	8.4
Uranium	No. of observations	Min.	Max.	Q1	Median	Q3	Inter-quartile range	Average	Std-dev.	Skewness	Kurtosis
Whole population	328	0.01	280	0.66	2.0	4.4	3.7	4.9	17	14	210
Cold-volcanic	223	0.01	85	1.3	2.8	5.4	4.2	6.0	8.2	5.6	43
Cold-sedimentary	57	0.07	22	0.57	1.1	2.7	2.2	2.5	3.9	3.3	12
Thermal waters	33	0.17	13	0.05	0.12	0.45	0.40	0.91	2.4	4.0	16
Bubbling pools	15	0.01	276	0.03	0.12	1.5	1.5	21	69	3.4	9.8
Vanadium	No. of observations	Min.	Max.	Q1	Median	Q3	Inter-quartile range	Average	Std-dev.	Skewness	Kurtosis
Whole population	302	0.05	350	2.8	8.9	15	12	12	24	10	130
Cold-volcanic	214	0.17	62	7.4	12	16	8.6	13	8.8	2.3	8.5
Cold-sedimentary	45	0.05	24	0.36	0.70	2.9	2.5	2.9	4.9	2.6	7.0
Thermal waters	33	0.08	17	0.25	0.42	0.98	0.73	1.5	3.2	3.8	15
Bubbling pools	10	0.05	350	0.68	11	140	130	73	110	1.6	1.3

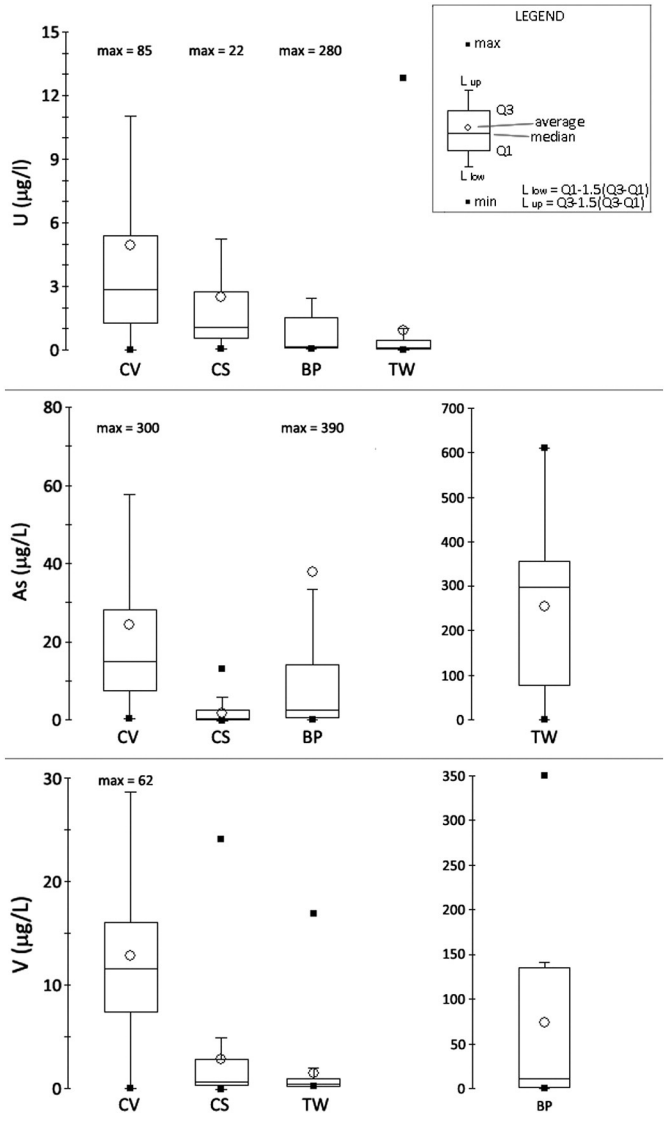

Fig. 2. Box plot of the subsets of the whole sampling population for As, U and V.

8.6 µg/L), with none of them exceeding the Italian limit value (120 µg/L) for drinking waters. The Levene's test (not shown) and the non-parametric Kruskal–Wallis method (see as electronic Supplementary material SM 4) were used for the statistical validation of the aforesaid differences among subsets, indicating that almost all groups are significantly dissimilar each other as regards to the selected elements.

4.2. Geostatistical analysis

Since the As, U and V concentrations exhibit non-normal distributions, i.e. the assumption of statistical normality was not initially satisfied, a Box–Cox transformation (Box and Cox, 1962) was applied in order to obtain a data distribution close to a Gaussian-type. Moreover some outliers were manually removed from the datasets in order to obtain more regular and interpretable variograms during the variographic analysis. For each transformed variable a directional semi-variogram was calculated for estimating the spatial variation of values of the regionalized variables (Figs. 3–5). A lag distance of 2000 m (tolerance ±1000 m) was used, which is comparable to the average minimum distance among sample pairs. This representation takes into account the anisotropy of the variables and allows the verification of the presence of spatial autocorrelation among experimental data and differences with respect to the two main directions considered for each variable. The common features of directional semi-variograms are the general increase of the semi-variance $\gamma(h)$ with the distance, within a specific radius of influence, while over that distance (*range*) the $\gamma(h)$ value remains approximately constant (*sill*), i.e. close to the variance of the variable. This means that a spatial correlation among observations exists within the range distance, over which no spatial correlation between data is apparent. Moreover, for $h = 0$ is the semi-variance $\gamma(h) > 0$ is not zero as it should be expected, due to the short scale variations enclosed within the first lag (nugget effect).

The geometric anisotropy for As is defined along N140°E and N230°E directions (Fig. 3), which were identified as representative of major (u direction) and minor axes (v direction) of anisotropy ellipse, respectively. In detail, the major axis is the direction of maximum spatial continuity of the variable (maximum range: 22,000 m) and the minor axis is the direction of maximum spatial variability (minimum range: 19,000 m). For U, the principal directions of the geometric anisotropy are N75°E and N165°E for maximum continuity (u direction, range 10,000 m) and maximum variability (v direction, range 9500 m), respectively (Fig. 4). For V, the geometric anisotropy was recognized along directions N100°E and N190°E for u (range 17,000 m) and v directions (range

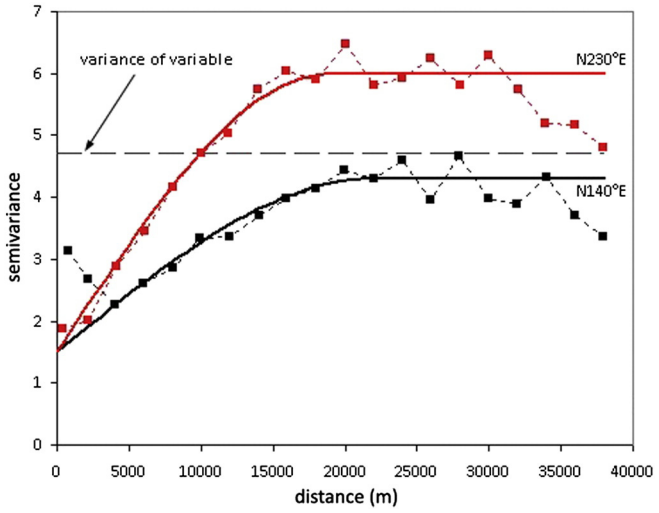

Fig. 3. Experimental directional semi-variogram of the Box–Cox-transformed As concentrations for the sampled waters.

11,000 m), respectively (Fig. 5). Model parameters and cross-validation results for As, U and V are reported as Supplementary material (SM 5).

Ordinary kriging was applied to produce estimation maps from Box–Cox variables, by using model parameters reported in SM 5. At a preliminary phase maps were back-transformed into original variable values, then they were edited manually in order to adjust the areas where outliers were removed from the dataset during the preliminary variographic analysis.

5. Discussion

5.1. Arsenic

The contour map of As concentration in groundwater calculated by using the variogram model parameters is shown in Fig. 6. The As distribution in groundwater is quite similar to those reported in previous investigations (Angelone et al., 2009; Baiocchi et al., 2013), although the larger dataset produced in this study and the homogeneous distribution of the sampling sites over the study area allowed a more detailed definition of boundaries between naturally contaminated areas (where As >10 μg/L) and areas where the As concentrations were below the threshold limit.

The As concentration in groundwater seems to be mainly influenced by water–rock interaction processes involving volcanic and sedimentary formations and locally enhanced by thermalism and the presence of acidic gas species (CO_2 and H_2S). The waters hosted in the permeable levels of the sedimentary units, mostly discharging in the N-eastern and S-western sectors of the study area (Fig. 6), show concentration values significantly lower than those emerging from the volcanic aquifer and generally <5 μg/L (Fig. 2). Conversely, the waters circulating in the volcanic aquifer show significant variations in terms of As concentrations with values ranging from 0.17 to 300 μg/L (Table 1). Concentrations generally <10 μg/L were measured in the Cimini Dome area and follow the flow path in the NE direction towards the Tevere valley. These values are probably due to *i*) relatively fast water circulation and short fluid pathways through the volcanic rocks, resulting in a limited water–rock interaction, and *ii*) lack of lateral groundwater inflow from other sectors. The occurrence of high As concentrations in other sectors of the volcanic aquifer is mainly related to the uprising of fluids from the hydrothermal reservoir and the local hydrostratigraphy, structural setting, and lateral flow discharge. The highest As concentrations resulted in a large area approximately WNW–ESE oriented (Fig. 6) extending from Tuscania to Nepi, and culminating with the notable N10°E-trending (10 km-long) alignment W of Viterbo (Fig. 1), where thermal springs and wells fed with temperatures up to 63 °C (Cinti et al., 2014) show values significantly higher than 100 μg/L. The presence of thermal fluids significantly increases the removal of As from the hosting rocks, due to the enhanced solubility of the solid phases during water–rock interaction processes at high temperatures (Ballantyne and Moore, 1988; Webster and Nordstrom, 2003). Consistently, deep-originated thermal waters are characterized by higher (from one to up to three orders of magnitude) As concentrations than those measured in the shallow cold waters (Table 1; Fig. 2). Significantly lower As concentrations were measured for those thermal waters which circulate within the sedimentary units (i.e. Orte sector) or where the volcanic cover shows a reduced thickness, e.g. in the southern of Capranica (Fig. 1), This suggests that As dissolution mainly occurs during the ascent of hydrothermal fluids and it is produced by water–rock interaction processes involving the volcanic As-rich rocks.

The hydrothermal fluids are preferentially upraising to the surface along extensional faults and fractured zones, suggesting the pivotal role played by the structural framework on the As spatial distribution. These faults border the buried structural highs of the pre-volcanic basement (Barberi et al., 1994), in a sector where the top of the hydrothermal reservoir is located at shallower depths (Cataldi et al., 1995) and a reduced thickness of the low-permeability sedimentary units occurs

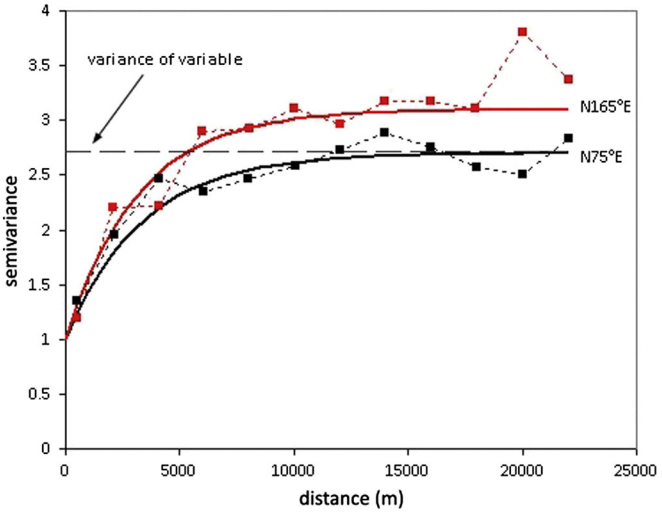

Fig. 4. Experimental directional semi-variogram of the Box–Cox-transformed U concentrations for the sampled waters.

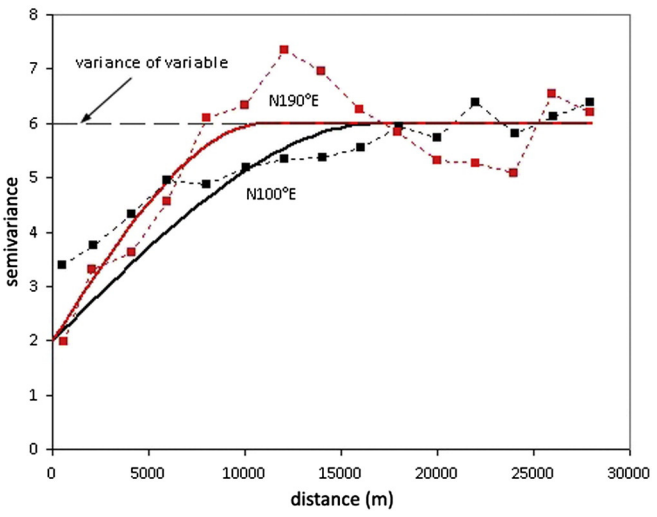

Fig. 5. Experimental directional semi-variogram of the Box–Cox-transformed V concentrations for the sampled waters.

Please cite this article as: Cinti, D., et al., Spatial distribution of arsenic, uranium and vanadium in the volcanic-sedimentary aquifers of the Vicano–Cimino Volcanic Distric..., J. Geochem. Explor. (2015), http://dx.doi.org/10.1016/j.gexplo.2015.02.008

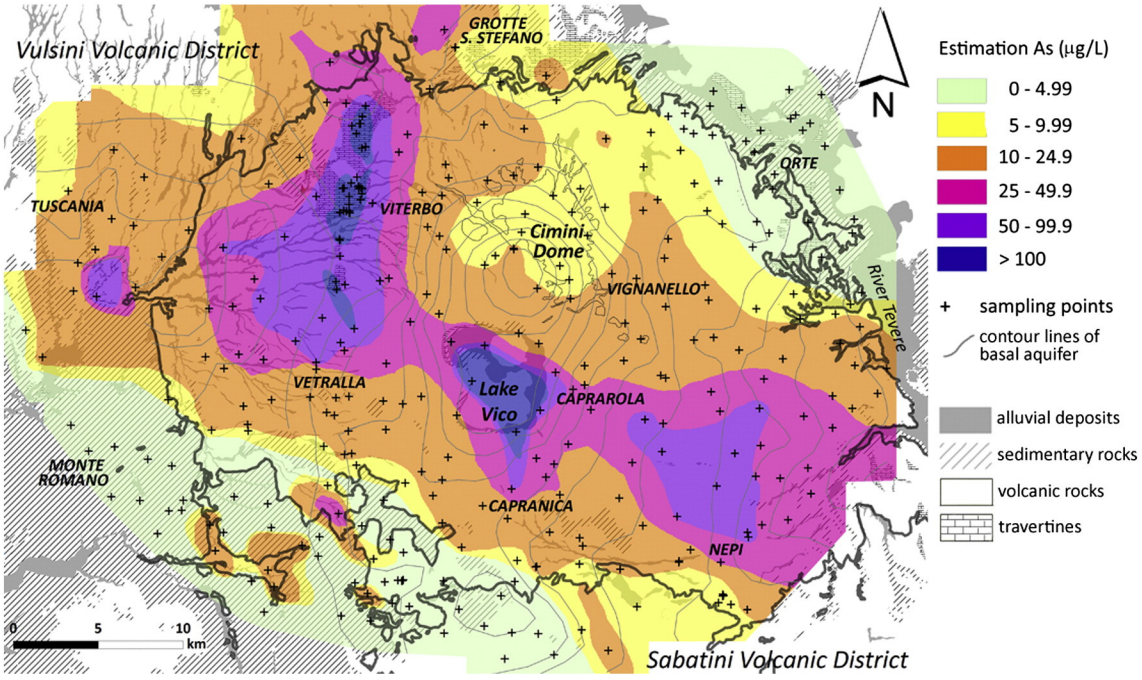

Fig. 6. Dissolved As iso-concentrations (µg/L) map in the VCVD as obtained from ordinary kriging after back-transformation and manual editing of extreme values (outliers).

(see profile of Fig. 1), favouring mixing phenomena between the deep-rising fluids and the shallow cold volcanic waters. The spatial distribution of As is consistent with the direction of the main structural elements (Barberi et al., 1994). This confirms that its highest concentrations are intimately related to those areas where the deep hydrothermal reservoir is uplifted under a reduced thickness of low-permeability units. Conversely, where fluids showed no relation with the structural framework, relatively low As concentrations were found (i.e. Cimini Dome area; Fig. 6). The top of the hydrothermal reservoir is indeed located at deeper depths in correspondence with large structural lows of the pre-volcanic basement (Barberi et al., 1994) and is filled by thick sequences of low-permeability sedimentary units (see profile in Fig. 1), which provide a natural barrier and hinder the mixing between shallow and deep fluids. It is worth noting that the high As concentrations (>10 µg/L) measured in such theoretically not contaminated sectors (i.e. Vignanello area; Fig. 6) were produced by lateral flow of As-rich waters related to well overexploitation, which has likely caused an enhanced vertical hydraulic gradient. Available data on water consumption for human activities (Baiocchi et al., 2013) suggest that the sector of Vignanello is one of the areas with the highest percentage of withdrawal from the basal aquifer, confirming the possibility that lateral inflow of As-rich waters occurs from the southern sector (Fig. 6).

As far as the distribution of As species is concerned, the Eh-pH diagram (Fig. 7) shows that under oxidizing conditions characterizing most of the cold waters the predominant species is the pentavalent As(V), which is mainly present as aqueous complex ($HAsO_4^{2-}$ and $H_2AsO_4^-$). Conversely, the trivalent form As(III), chiefly occurring as non-ionic species ($HAsO_2$), is the thermodynamically stable form for most thermal waters and bubbling pools.

5.2. Uranium

Uranium concentrations in groundwater (Fig. 8) were <5 µg/L, with the exception of two approximately NE–SW oriented areas located S of Tuscania and between Capranica and Caprarola, respectively, and some isolated samples mainly located N of Viterbo. Despite the well documented high U contents of lavas and pyroclastic deposits of the volcanic provinces of northern Latium (Locardi and Mittempergher, 1971; Locardi and Sircana, 1967) and the significantly lower U contents of the sedimentary units (Trevisi et al., 2005), waters circulating in the volcanic units are only slightly enriched in U with respect to those emerging from the sedimentary deposits (Figs. 2, 8). This is probably due to the relatively low U mobility, since this element is typically enriched in minerals resistant to alteration, such as the monazite group (Locardi and Battistella, 1987). Uranium dissolution from the volcanic rocks is responsible for the formation of the U mineral deposits recognized in the volcanic provinces of northern Latium. These mineralized areas are characterized by occurrence of U oxides in supergene-altered volcanic rocks that are converted into kaolin and opal and veined with dispersed iron sulphides (Locardi and Battistella, 1987; Locardi and Mittempergher, 1971). The mineralized areas are always associated with acidic gas exhalations (CO_2, H_2S) fed by the active

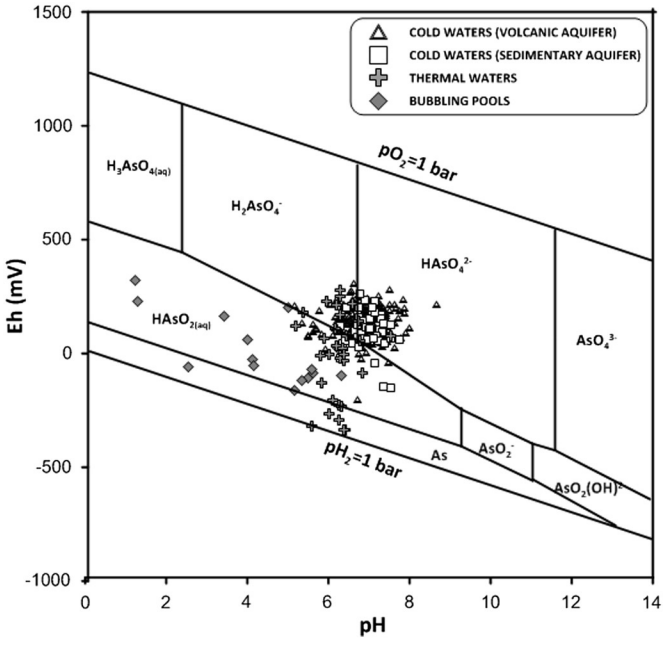

Fig. 7. Eh–pH diagram of As species in the As–O_2–H_2O system.

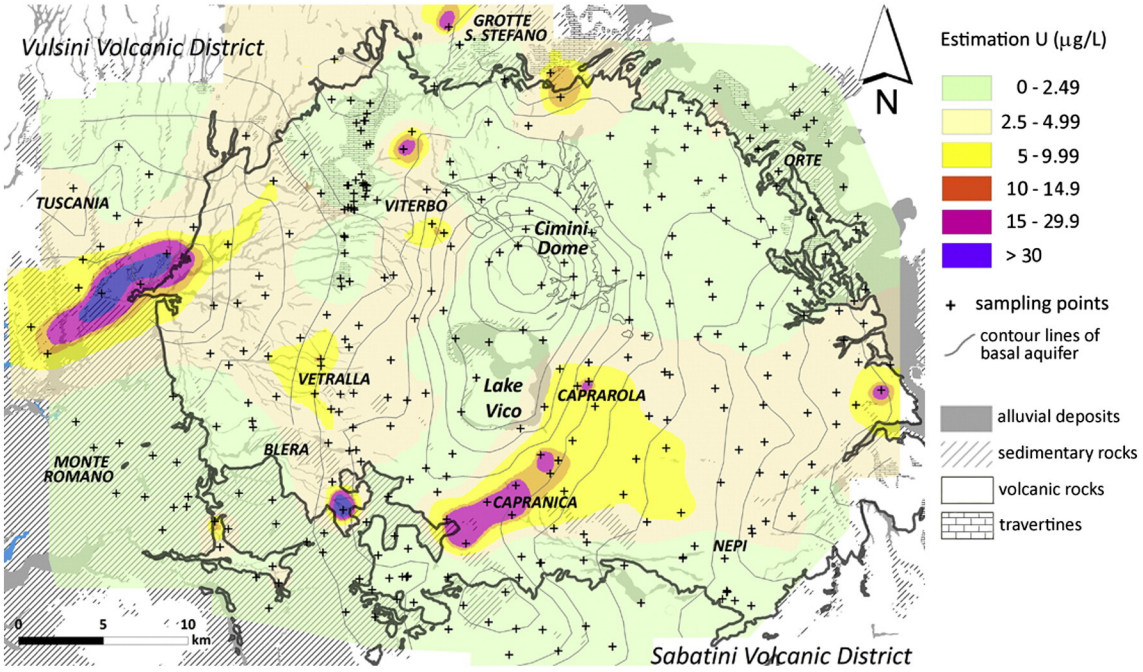

Fig. 8. Dissolved U iso-concentrations (µg/L) map in the VCVD as obtained from ordinary kriging after back-transformation and manual editing of extreme values (outliers).

hydrothermal reservoir. These gases, in particular H_2S, favour U dissolution during water–gas–rock interaction involving volcanic rocks, and produce favourable pH–Eh (i.e. reducing) conditions for U precipitation, mainly as UO_2, in the supergene environment (Locardi and Battistella, 1987; Locardi and Mittempergher, 1971). Redox conditions strongly control U concentrations in waters, due to the large difference of solubility between U(VI) and U(IV) species (Fig. 9) (Smedley et al., 2006). Widespread uranium mineralized areas in the N-western sector of VCVD, between Tuscania, Viterbo and Grotte S. Stefano (Locardi and Battistella, 1987) and in the Capranica area (Capannesi et al., 2012; Rossi et al., 1995) are fairly overlapping with the highest U concentrations in groundwater (Fig. 8). This implies that U is more efficiently leached from these mineral deposits, through supergene oxidative alteration, rather than from the minerals of the volcanic rocks.

The Eh–pH diagram (Fig. 9) calculated in the absence of ligands other than hydroxide shows that cold waters are mostly characterized by nearly-neutral and oxidizing conditions, favouring the U mobility through the formation of soluble anionic carbonate complexes, such as $UO_2(CO_3)^{2-}$ (Smedley et al., 2006), that decrease U-adsorption on mineral surfaces. Conversely, the prevailing anoxic conditions of most thermal waters and bubbling pools in the study area strongly decrease the U mobility due its precipitation. Consistently, relatively high U concentrations characterized the cold waters both from volcanic and sedimentary aquifers, while significantly lower concentrations were measured in the thermal and bubbling waters (Fig. 2). Uranyl ion (UO_2^{2+}) was the dominant species in low-pH (<5) bubbling pools, whereas sulphate and fluoride complexes likely prevail at pH values less than 3 (Smedley et al., 2006).

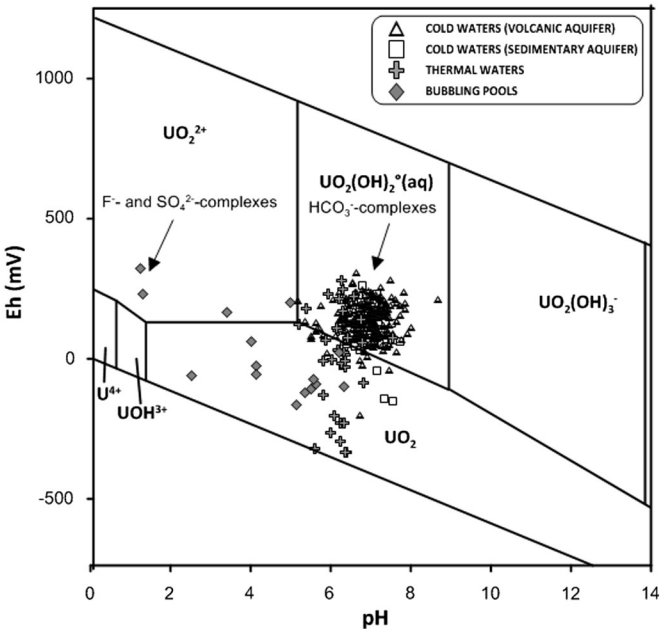

Fig. 9. Eh–pH diagram of U species in the U–O_2–H_2O system.

5.3. Vanadium

The contour map of V in groundwater is shown in Fig. 10. As for As and U, waters hosted in the volcanic rocks show higher concentrations than those circulating in the sedimentary units (Fig. 2). This is consistent with the relatively high V contents in the groundmass of the volcanic rocks of the VCVD (up to 255 ppm; Aulinas et al., 2011; Perini et al., 2004), where V^{3+} can substitute Fe^{3+} in the mineral structure of pyroxene and magnetite (Nriagu, 1998). Vanadium is also contained in some V-rich minerals (i.e. carnotite and vanadinite) that commonly occur in the volcanic rocks of northern Latium as secondary minerals and/or in the mineralized areas mainly in association with U (Della Ventura et al., 1999; Locardi and Battistella, 1987; Parodi et al., 1989). The spatial distribution of the V concentrations of waters circulating in the volcanic aquifer shows significant variations between the central sector, including the Cimini Dome and the Lake Vico caldera, which is characterized by lower values and the peripheral areas where higher values occur (Fig. 10). These differences are probably related to the radially divergent flow of the volcanic aquifer controlling the length of the flow path and producing an efficient leaching of the volcanic rocks in the distal areas, due to prolonged time of water–rock interaction.

Please cite this article as: Cinti, D., et al., Spatial distribution of arsenic, uranium and vanadium in the volcanic-sedimentary aquifers of the Vicano–Cimino Volcanic Distric..., J. Geochem. Explor. (2015), http://dx.doi.org/10.1016/j.gexplo.2015.02.008

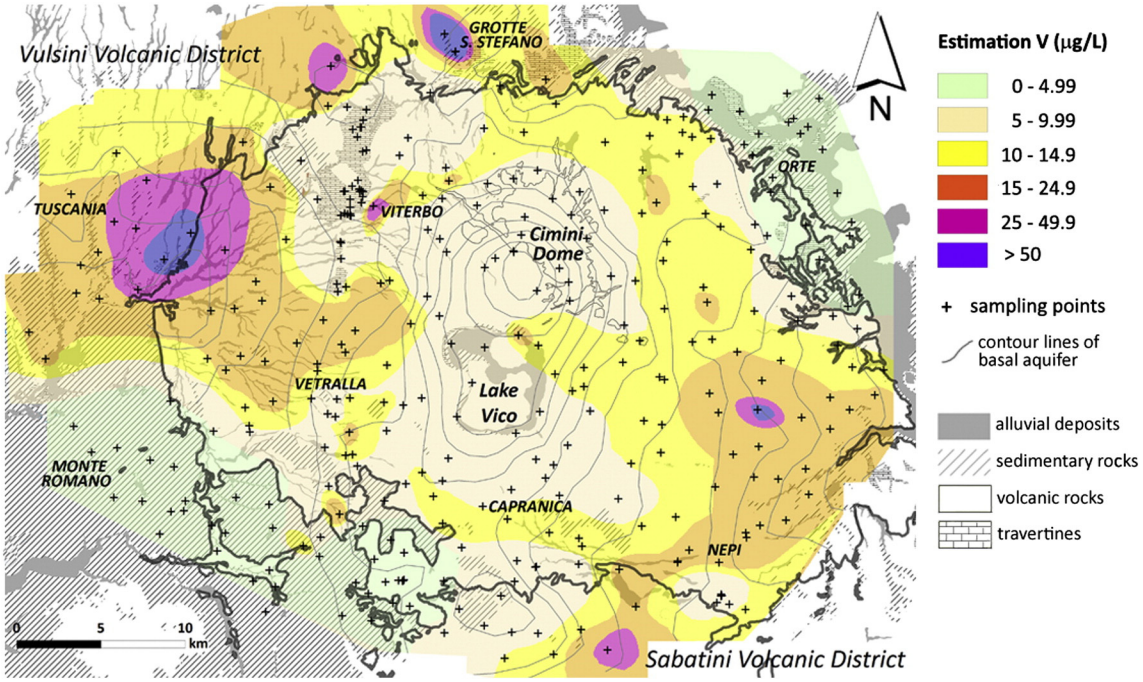

Fig. 10. Dissolved V iso-concentrations (µg/L) map in the VCVD as obtained from ordinary kriging after back-transformation and manual editing of extreme values (outliers).

Vanadium mobility in natural waters mainly depends on oxidation state, pH conditions and the tendency to form anionic complexes (Nriagu, 1998). Consistently, the Eh–pH diagram for V aqueous species in the system V–O–H (Fig. 11) shows that under oxidizing and nearly neutral conditions characterizing the cold waters and some thermal waters the formation of highly soluble V(V) oxy-anion $H_2VO_4^-$ is favoured. Conversely, the V(III) oxy-cation $V(OH)_2^+$ is predicted to be the dominant species for thermal waters under reducing conditions. V(III) rapidly hydrolyzes in solution forming relatively insoluble oxy-hydroxides (Nriagu, 1998), as testified by the very low V concentrations found in thermal waters (Fig. 2). Under oxidizing and acidic (pH < 4) conditions typical of many bubbling pools the highly soluble V(IV) oxy-cation VO^{2+} is predominant.

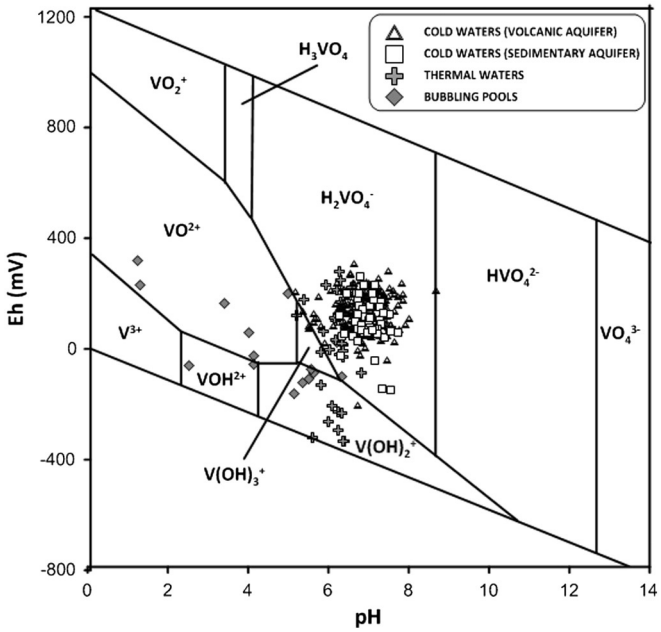

Fig. 11. Eh–pH diagram of V species in the $V–O_2–H_2O$ system.

6. Conclusions

The contour maps of As, U, and V concentrations in groundwater were obtained on the basis of analytical data of wells and springs collected during a detailed sampling survey carried out in the VCVD by applying a geostatistical approach, with the aim of establishing the source of those potentially toxic trace elements and defining the main factors controlling their distribution.

Rock composition is considered to be the main factor controlling the higher As concentrations measured in waters discharging from the volcanic rocks relative to those circulating within the sedimentary deposits, due to the high As content in the groundmass of lavas and pyroclastites.

Within the volcanic aquifer, the spatial distribution of As is not homogeneous, being controlled by the structural assessment of VCVD. Relatively high As concentrations were measured in correspondence of fractured and faulted zones, i.e. in sectors characterized by reduced thickness of low-permeability cap units favouring the discharge of the hydrothermal fluids and, consequently, enhancing mineral solubility during water–rock interaction processes. Conversely, where the volcanic and the hydrothermal aquifer are isolated, relatively low As concentrations were measured.

Relatively high U and V concentrations were determined in groundwater circulating within the volcanic rocks relative to the sedimentary units. Higher concentrations also occurred in correspondence with U and V mineralized areas within the volcanic complexes. The mobilization of U and V is favoured at oxidizing condition and nearly neutral pH, typical of shallow aquifers, whereas under anoxic conditions, characterizing the deep environment sourcing thermal waters, relatively insoluble species prevailed.

Geochemical mapping represents a valid and solid tool for a more accurate management of the water resources of an area where they supply the local demand of drinking water for about 170,000 inhabitants. The results of the present study suggest that hydrothermal and faulted areas are the more vulnerable sites from where drinking water is still pumped. In general, the extension of the As-contaminated sectors, as derived by kriging, nearly covers 60% of the study area, suggesting that new hydrogeological investigations should be oriented in the SW and NE portions to exploit a good water quality in terms of As

Please cite this article as: Cinti, D., et al., Spatial distribution of arsenic, uranium and vanadium in the volcanic-sedimentary aquifers of the Vicano–Cimino Volcanic Distric..., J. Geochem. Explor. (2015), http://dx.doi.org/10.1016/j.gexplo.2015.02.008

concentrations. Furthermore, a sustainable and efficient water management should take into account the possible negative effects produced by well overexploitation, associated with high pumping rates from wells, which can move naturally contaminated waters, by vertical and lateral inflow, towards less affected areas.

As regards to U and V, the risk posed by natural contamination of water resources is, at present, very low.

Supplementary data to this article can be found online at http://dx.doi.org/10.1016/j.gexplo.2015.02.008.

Acknowledgements

Many thanks are due to two anonymous reviewers for their constructive comments and suggestions that allowed us to substantially improve an early version of this paper.

References

Aiuppa, A., Avino, R., Brusca, L., Caliro, S., Chiodini, G., D'Alessandro, W., Favara, R., Federico, C., Ginevra, W., Inguaggiato, S., Longo, M., Pecoraino, G., Valenza, M., 2006. Mineral control of arsenic content in thermal waters from volcano-hosted hydrothermal systems: insights from island of Ischia and Phlegrean Fields (Campanian Volcanic Province, Italy). Chem. Geol. 229, 313–330.

Angelone, M., Cremisini, C., Piscopo, V., Proposito, M., Spaziani, F., 2009. Influence of hydrostratigraphy and structural setting on the arsenic occurrence in groundwater of the Cimino-Vico volcanic area (central Italy). Hydrogeol. J. 17, 901–914.

Aulinas, M., Gasperini, D., Gimeno, D., Macera, P., Fernandez-Turiel, J.L., Cimarelli, C., 2011. Coexistence of calc-alkaline and ultrapotassic alkaline magmas at Mounts Cimini: evidence for transition from the Tuscan to the Roman Magmatic Provinces. Geol. Acta 9, 103–125.

Baiocchi, A., Dragoni, W., Lotti, F., Luzzi, G., Piscopo, V., 2006. Outline of the hydrogeology of the Cimino and Vico volcanic area and of the interaction between groundwater and lake Vico (Lazio Region, central Italy). Boll. Soc. Geol. Ital. 125, 187–202.

Baiocchi, A., Coletta, A., Espositi, L., Lotti, F., Piscopo, V., 2013. Sustainable groundwater development in a naturally arsenic-contaminated aquifer: the case of the Cimino-Vico volcanic area (central Italy). Ital. J. Eng. Geol. Environ. http://dx.doi.org/10.4408/IJEGE.2013-01.O-01.

Ballantyne, J.M., Moore, J.N., 1988. Arsenic geochemistry in geothermal systems. Geochim. Cosmochim. Acta 52, 475–483.

Barberi, F., Buonasorte, G., Cioni, R., Fiordelisi, A., Foresi, L., Iaccarino, S., Laurenzi, M.A., Sbrana, A., Vernia, L., Villa, I.M., 1994. Plio-Pleistocene geological evolution of the geothermal area of Tuscany and Latium. Mem. Descr. Carta Geol. Ital. 49, 77–134.

Box, G.E.P., Cox, D.R., 1962. An analysis of transformations. J. R. Stat. Soc. Ser. B 26, 211–252.

Brown, M.B., Forsythe, A.B., 1974. Robust tests for the equality of variance. J. Am. Stat. Assoc. 69, 364–367.

Capannesi, G., Rosada, A., Manigrasso, M., Avino, P., 2012. Rare earth elements, thorium and uranium in ores of the North-Latium (Italy). J. Radioanal. Nucl. Chem. 291, 163–168.

Capelli, G., Mazza, R., Gazzetti, C., 2005. Strumenti e strategie per la tutela e l'uso compatibile della risorsa idrica nel Lazio: gli acquiferi vulcanici. Ed. Pitagora.

Cataldi, R., Mongelli, F., Squarci, P., Taffi, L., Zito, G., Calore, C., 1995. Geothermal ranking of Italian territory. Geothermics 24, 115–129.

Chiodini, G., Frondini, F., Kerrick, D.M., Rogie, J., Parello, F., Peruzzi, L., Zanzari, A.R., 1999. Quantification of deep CO_2 fluxes from central Italy. Examples of carbon balance for regional aquifers and of soil diffuse degassing. Chem. Geol. 159, 205–222.

Cicchella, D., Albanese, S., De Vivo, B., Dinelli, E., Giaccio, L., Lima, A., Valera, P., 2010. Trace elements and ions in Italian bottled mineral waters: identification of anomalous values and human health related effects. J. Geochem. Explor. 107, 336–349.

Cimarelli, C., De Rita, D., 2006. Structural evolution of the Pleistocene Cimini trachytic volcanic complex (Central Italy). Bull. Volcanol. 68, 538–548.

Cinti, D., Tassi, F., Procesi, M., Bonini, M., Capecchiacci, F., Voltattorni, N., Vaselli, O., Quattrocchi, F., 2014. Fluid geochemistry and geothermometry in the unexploited geothermal field of the Vicano–Cimino volcanic district (central Italy). Chem. Geol. 371, 96–114.

Crebelli, R., Leopardi, P., 2012. Long-term risks of metal contaminants in drinking water: a critical appraisal of guideline values for arsenic and vanadium. Ann. Ist. Super. Sanità 48, 354–361.

Dall'Aglio, M., Giuliano, G., Amicizia, D., Andrenelli, M.C., Cicioni, G.B., Mastroianni, D., Sepicacchi, L., Tersigni, S., 2001. Assessing drinking water quality in northern Latium by trace elements analysis. In: Cidu, R. (Ed.), Proc. of the 10th Int. Symp. on Water–Rock Interaction, Villasimius, Italy, pp. 1063–1066.

Della Ventura, G., Bellatreccia, F., Caprilli, E., Rossi, P., Fiori, S., 1999. Minerali di vanadio nei prodotti sienitici del Lazio: la vanadinite di Monte Cavalluccio, Campagnano (Roma). Rend. Fis. Acc. Lincei 10, 81–87.

Dinelli, E., Lima, A., De Vivo, B., Albanese, S., Cicchella, D., Valera, P., 2010. Hydrogeochemical analysis on Italian bottled mineral waters: effects of geology. J. Geochem. Explor. 107, 317–335.

Dinelli, E., Lima, A., Albanese, S., Birke, M., Cicchella, D., Giaccio, L., Valera, P., De Vivo, B., 2012. Major and trace elements in tap water from Italy. J. Geochem. Explor. 112, 54–75.

EC Directive, 1998. Council Directive 98/83/EC of 3 November 1998 on the Quality of Water Intended for Human Consumption. European Commission, Brussels.

EFSA (European Food Safety Authority), 2009. Uranium in foodstuffs, in particular mineral water. Scientific opinion of the panel on contaminants in the food chain. EFSA J. 1018, 1–59.

Frengstad, B., Midtgård Skrede, A.K., Banks, D., Krog, J.R., Siewers, U., 2000. The chemistry of Norwegian groundwaters: III. The distribution of trace elements in 476 crystalline bedrock groundwaters, as analysed by ICP-MS techniques. Sci. Total Environ. 246, 21–40.

Gerke, T.L., Scheckel, K.G., Maynard, J.B., 2010. Speciation and distribution of vanadium in drinking water iron pipe corrosion by-products. Sci. Total Environ. 408, 5845–5853.

Giammanco, S., Valenza, M., Pignato, S., Giammanco, G., 1996. Mg, Mn, Fe and V concentrations in the ground waters of mount Etna (Sicily). Water Res. 30, 378–386.

Goovaerts, P., 1997. Geostatistics for Natural Resources Evaluation. Oxford University Press, New York.

IARC (International Agency for Research on Cancer), 2004. IARC monographs on the evaluation of carcinogenic risks to humans. Volume 84. Some drinking-water disinfectants and contaminants, including arsenic (Lyon).

Katsoyiannis, I.A., Hug, S.J., Ammann, A., Zikoudi, A., Hatziliontos, C., 2007. Arsenic speciation and uranium concentrations in drinking water supply wells in northern Greece: correlations with redox indicative parameters and implications for groundwater treatment. Sci. Total Environ. 383, 128–140.

Kruskal, W.H., Wallis, W.A., 1952. Use of ranks in one-criterion variance analysis. J. Am. Stat. Assoc. 47, 583–621.

Laurenzi, M.A., Villa, I.M., 1987. $^{40}Ar/^{39}Ar$ chronostratigraphy of Vico ignimbrites. Period. Mineral. 56, 285–293.

Locardi, E., Battistella, F., 1987. Distribuzione dell'uranio, torio, fluoro e berillo nella provincia tosco-laziale. L'Industria Mineraria 2, 5–20.

Locardi, E., Mittempergher, M., 1971. Exhalative supergenic uranium, thorium and marcasite occurrences in quaternary volcanites of central Italy. Bull. Volcanol. 35, 173–184.

Locardi, E., Sircana, S., 1967. Distribuzione dell'uranio e del torio nelle vulcaniti alcaline del Lazio settentrionale. Rend. Soc. Min. Ital. 23, 163–224.

Milvy, P., Cothern, R., 1990. Scientific background for the development of regulations for radionuclides in drinking water. In: Cothern, R., Rebers, P. (Eds.), Radon, Radium, and Uranium in Drinking Water, pp. 1–16.

Minissale, A., 2004. Origin, transport and discharge of CO_2 in Central Italy. Earth-Sci. Rev. 66, 89–141.

Nicoletti, M., 1969. Datazioni argon-potassio di alcune vulcaniti delle regioni vulcaniche Cimina e Vicana. Period. Mineral. 38, 1–20.

Nriagu, J., 1998. History, occurrence, and use of vanadium. In: Nriagu, J. (Ed.), Vanadium in the Environment, Part 1: Chemistry and Biochemistry. John Wiley & Sons, Inc., New York, pp. 1–24.

Nriagu, J., Nam, D.-H., Ayanwola, T.A., Dinh, H., Erdenechimeg, E., Ochir, C., Bolormaa, T.-A., 2012. High levels of uranium in groundwater of Ulaanbaatar, Mongolia. Sci. Total Environ. 414, 722–726.

Parodi, G.C., Della Ventura, G., Lorand, J.P., 1989. Mineralogy and petrology o fan unusual osumilite + vanadium-rich pseudobrookite assemblage in an ejectum from the Vico Volcanic Complex (Latium, Italy). Am. Mineral. 74, 1278–1284.

Peccerillo, A., 1985. Roman comagmatic province: evidence for subduction-related magma genesis. Geology 13, 103–106.

Perini, G., Francalanci, L., Davidson, J.P., Conticelli, S., 2004. Evolution and genesis of magmas from Vico volcano, central Italy: multiple differentiation pathways and variable parental magmas. J. Petrol. 45, 139–182.

Pourret, O., Dia, A., Gruaua, G., Davranche, M., Bouhnik-Le Coz, M., 2012. Assessment of vanadium distribution in shallow groundwaters. Chem. Geol. 294–295, 89–102.

Rahman, M.M., Sengupta, M.K., Ahamed, S., Chowdhury, U.K., Hossain, M.A., Das, B., Lodh, D., Saha, K.C., Pati, S., Kaies, I., Barua, A.K., Chakraborti, D., 2005. The magnitude of arsenic contamination in groundwater and its health effects to the inhabitants of the Jalangi: one of the 85 arsenic affected blocks in West Bengal, India. Sci. Total Environ. 338, 189–200.

Romero, L., Alonso, H., Campano, P., Fanfani, L., Cidub, R., Dadea, C., Keegan, T., Thornton, I., Farago, M., 2003. Arsenic enrichment in waters and sediments of the Rio Loa (Second Region, Chile). Appl. Geochem. 18, 1399–1416.

Rossi, P., Bellatreccia, F., Caprilli, E., Parodi, G.C., Della Ventura, G., Mottana, A., 1995. A new occurrence of rare minerals in anejectum in the pyroclastics of VicoVolcano, Roman Comagmatic Region, Italy. Rend. Fis. Acc. Lincei 6, 147–156.

Scrocca, D., Doglioni, C., Innocenti, F., 2003. Constraints for an interpretation of the Italian geodynamics: a review. Mem. Descr. Carta Geol. Ital. 62, 15–46.

Smedley, P.L., Kinniburgh, D.G., 2002. A review of the source, behavior and distribution of arsenic in natural waters. Appl. Geochem. 17, 517–568.

Smedley, P.L., Kinniburgh, D.G., Macdonald, D.M.J., Nicolli, H.B., Barros, A.J., Tullio, J.O., Pearce, J.M., Alonso, M.S., 2005. Arsenic associations in sediments from the loess aquifer of La Pampa, Argentina. Appl. Geochem. 20, 989–1016.

Smedley, P.L., Smith, B., Abesser, C., Lapworth, D., 2006. Uranium occurrence and behavior in British groundwater. British Geological Survey [Report No.: CR/06/050/N].

Sollevanti, F., 1983. Geologic, volcanologic, and tectonic setting of the Vico-Cimino area, Italy. J. Volcanol. Geotherm. Res. 17, 203–217.

Spadoni, M., Voltaggio, M., Cavarretta, G., 2005. Recognition of areas of anomalous concentration of potentially hazardous elements by means of a subcatchment-based discriminant analysis of stream sediments. J. Geochem. Explor. 87, 83–91.

Tamasi, G., Cini, R., 2004. Heavy metals in drinking waters from Mount Amiata (Tuscany, Italy). Possible risks from arsenic for public health in the Province of Siena. Sci. Total Environ. 327, 41–51.

Please cite this article as: Cinti, D., et al., Spatial distribution of arsenic, uranium and vanadium in the volcanic-sedimentary aquifers of the Vicano–Cimino Volcanic Distric..., J. Geochem. Explor. (2015), http://dx.doi.org/10.1016/j.gexplo.2015.02.008

Trevisi, R., Bruno, M., Orlando, C., Ocone, R., Paolelli, C., Amici, M., Altieri, A., Antonelli, B., 2005. Radiometric characterization of more representative natural building materials in the province of Rome. Radiat. Prot. Dosim. 113, 168–172.

U.S. Environmental Protection Agency, 2009. Fact Sheet: Final 3rd Drinking Water Contaminant Candidate List (CCL 3). http://water.epa.gov/scitech/drinkingwater/dws/ccl/upload/fs_cc3_final.pdf.

Villemant, B., Fléoch, C., 1989. U–Th fractionation by fluids in K-rich magma genesis: the Vico volcano, central Italy. Earth Planet. Sci. Lett. 91, 312–326.

Vivona, R., Preziosi, E., Madé, B., Giuliano, G., 2007. Occurrence of minor toxic elements in volcanic–sedimentary aquifers: a case study in central Italy. Hydrogeol. J. 15, 1183–1196.

Webster, J.G., Nordstrom, D.K., 2003. Geothermal arsenic. In: Welch, A.H., Stollenwerk, K.G. (Eds.), Arsenic in Groundwater, Geochemistry and Occurrence. Kluvert, The Netherlands, pp. 101–112.

WHO, 2011. Guidelines for Drinking-Water Quality. 4th ed. WHO Press, Geneva.

Wright, M.T., Stollenwerk, K.G., Belitz, K., 2014. Assessing the solubility controls on vanadium in groundwater, northeastern San Joaquin Valley, CA. Appl. Geochem. 48, 41–52.

Wu, Y., Wang, Y., Xie, X., 2014. Occurrence, behaviour and distribution of high levels of uranium in shallow groundwater at Datong basin, northern China. Sci. Total Environ. 472, 809–817.

Please cite this article as: Cinti, D., et al., Spatial distribution of arsenic, uranium and vanadium in the volcanic-sedimentary aquifers of the Vicano–Cimino Volcanic Distric..., J. Geochem. Explor. (2015), http://dx.doi.org/10.1016/j.gexplo.2015.02.008